Inorg. Chem. **2007**, *46*, 3865–3875

Cyclometallated Iridium and Platinum Complexes with Noninnocent Ligands

Bhavna Hirani,[†] Jian Li,[†] Peter I. Djurovich,[†] Muhammed Yousufuddin,[†] Jonas Oxgaard,[‡] Petter Persson,[§] Scott R. Wilson,[||] Robert Bau,[†] William A. Goddard III,[‡] and Mark E. Thompson*,[†]

Department of Chemistry, University of Southern California, Los Angeles, California 90089, Beckman Institute, California Institute of Technology, Pasadena, California 91106, Department of Chemical Physics, Lund University, Lund, Sweden, and Department of Chemistry, University of Illinois, Urbana, Illinois 61801

Received August 17, 2006

The electronic properties of the cyclometalated (C^N) complexes of iridium and platinum metals with a catechol ligand have been studied experimentally and computationally. The synthesis and characterization of (*p*-tolylpyridine)-Ir(3,5-di-*tert*-butylcatechol) (abbreviated Ir-sq) and (2,4-diflorophenylpyridine)Pt(3,5-di-*tert*-butylcatechol) (abbreviated Pt-sq) are reported along with their structural, spectral, and electrochemical properties. Reaction of the 3,5-di-*tert*-butylcatechol (DTBCat) ligand with the prepared cyclometalated metal complex was carried out in air in the presence of a base. The resulting complexes are air stable and are paramagnetic with the unpaired electron residing mainly on the catechol ligand. The bond lengths obtained from X-ray structure analysis and the theoretical results suggest the semiquinone form of the catechol ligand. Low-energy, intense ($\sim 10^3$ M^{-1} cm^{-1}) transitions are observed in the visible to near-infrared region (600–700 nm) of the absorption spectra of the metal complexes. Electrochemically, the complexes exhibit a reversible reduction of the semiquinone form to the catechol form of the ligand and an irreversible oxidation to the unstable quinone form of the ligand. The noninnocent catechol ligand plays a significant role in the electronic properties of the metal complexes. Density functional theory (DFT) and time-dependent density functional theory (TD-DFT) calculations on the two open-shell molecules provide the ground-state and excited-state energies of the molecular orbitals involved in the observed low-energy transitions. The spin density in the two complexes resides mainly on the catechol ligand. The intense transition arises from excitation of the β electron from a HOMO-*n* ($n = 1$ or 2 here) to the LUMO, rather than from the excitation of the unpaired α electron.

Introduction

Coordination chemistry of transition metal complexes of the redox active 1,2-dioxolene ligands has been extensively studied in the last 25 years.[1−6] Part of the interest in these complexes stems from the fact that the transition-metal orbitals and ligand frontier orbitals are close in energy resulting in strong mixing between these orbitals, such that the assignment of oxidation states to individual metal and ligand components is difficult. Such ligands are termed as "noninnocent" ligands.[1−6] The redox isomers of the ligands, shown in Scheme 1, exhibit potential for forming complexes that may exist in a number of electronic states because of the combined electrochemical activity of the metal and the ligand. The metal complexes show low-energy charge-transfer transitions that are fully allowed and thereby intense. They are also redox switchable, because the ligand can be readily interconverted between the different forms electrochemically.

A number of applications have been described, stemming from fundamental studies on noninnocent ligands and their metal complexes. Redox-switchable electrochromic dyes, for modulation of optical signals and smart windows, which selectively filter out infrared radiation from sunlight, are

* To whom correspondence should be addressed. E-mail: met@usc.edu.
[†] University of Southern California.
[‡] California Institute of Technology.
[§] Lund University.
[||] University of Illinois.

(1) Evangelio, E.; Ruiz-Molina, D. *Eur. J. Inorg. Chem.* **2005**, 3057.
(2) Hendrickson, D. N.; Pierpont, C. G. *Top. Curr. Chem.* **2004**, *234*, 63.
(3) Pierpont, C. G. *Coord. Chem. Rev.* **2001**, *219*−*221*, 415.
(4) Pierpont, C. G. *Coord. Chem. Rev.* **2001**, *216*−*217*, 99.
(5) Pierpont, C. G.; Lange, C. W. *Prog. Inorg. Chem.* **1994**, *41*, 331.
(6) Pierpont, C. G.; Buchanan, R. M. *Coord. Chem. Rev.* **1981**, *38*, 45.

10.1021/ic061556b CCC: $37.00
Published on Web 04/18/2007

Scheme 1

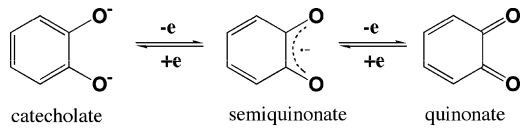

examples.[7−9] These materials could be useful in organic solar cells as near-IR sensitizers because of their strong absorption extending into the 700−900 nm region.[10,11] The spectroelectrochemical properties of ruthenium and osmium complexes with dioxolene ligands have been reported in detail.[12−15] Many of these complexes show intense, low-energy transitions that are redox switchable. The molecule with the low-energy transition has the semiquinone form of the dioxolene ligand coordinated to the metal center.

There are fewer reports on the electronic structures of open-shell platinum and iridium complexes of dioxolene ligands than there are on their Ru and Os counterparts. In the previous reports of Pt and Ir complexes of the dioxolene ligand, triarylphosphines or cyclooctadienes were used to fill out the metal coordination sphere.[16−18] The semiquinone form of the ligand was formed by chemical oxidation of the catecholate, and the complex was found to be unstable at room temperature, in some cases.[19,20] A stable platinum complex[16] formed by electrochemical oxidation of catecholate (diamagnetic) to the semiquinone (paramagnetic) form showed a red shift in absorbance. A square-planar bis(semiquinone) complex[21] of platinum(II) has also been studied that is diamagnetic and shows intense absorption bands in the near-infrared region. Platinum(II) complexes containing 2,2′-bipyridine as the chelating ligand and a chelated dithiolene/dioxolene ligand were reported as efficient and stable photosensitizers for singlet molecular oxygen production.[22,23] These complexes are neutral and diamagnetic. The catecholate form of a five-coordinate triphos-iridium(III) compound[24−26] has been studied for the uptake of dioxygen, both experimentally and theoretically. The electrochemical oxidation of this complex results in the semiquinone form of the ligand. A bis(catechol)-iridium(IV) complex[27] with a 1,5-cyclooctadiene ligand was characterized with an intense absorption band at very low energy.

Recently, a wide variety of iridium[28−38] and platinum[39−46] complexes with cyclometalated ligands have been reported as emissive materials in organic light-emitting diodes (OLEDs).[47,48] With the use of different cyclometalating ligands on the metal, we could possibly be able to optimize the electronic properties of the metal−dioxolene complex, giving materials that absorb at long wavelengths with high oscillator strengths.

We report here the synthesis and characterization of cyclometalated (C^N) complexes of iridium and platinum with 3,5-di-*tert*-butylcatechol (Figure 1). The electronic transitions and the electrochemical behavior of these open-shell molecules are presented here both from experimental observations and theoretical calculations.

(7) Mortimer, R. J. *Chem. Soc. Rev.* **1997**, *26*, 147.
(8) Rosseinsky, D. R.; Mortimer, R. J. *Adv. Mater.* **2001**, *13*, 783.
(9) Fablan, J.; Nakazumi, H.; Matsuoka, M. *Chem. Rev.* **1992**, *92*, 1197.
(10) Nazeeruddin, M. K.; Pechy, P.; Renouard, T.; Zakeeruddin, S. M.; Humphry-Baker, R.; Comte, P.; Liska, P.; Cevey, L.; Costa, E.; Shklover, V.; Spiccia, L.; Deacon, G. B.; Bignozzi, C. A.; Gratzel, M. *J. Am. Chem. Soc.* **2001**, *123* (8), 1613−1624.
(11) Peumans, P.; Yakimov, A.; Forrest, S. R. *J. Appl. Phys.* **2002**, *93*, 3693.
(12) Ward, M. D.; McCleverty, J. A. *J. Chem. Soc.* **2002**, 275.
(13) Haga, M.; Isobe, K.; Boone, S. R.; Pierpont, C. G. *Inorg. Chem.* **1990**, *29*, 3795.
(14) Haga, M.; Dodsworth, E. S.; Lever, A. B. P. *Inorg. Chem.* **1986**, *25*, 447.
(15) Schwab, P. F. H.; Diegoli, S.; Biancardo, M.; Bignozzi, C. A. *Inorg. Chem.* **2003**, *42*, 6613.
(16) Girgis, A. Y.; Sohn, Y. S.; Balch, A. L. *Inorg. Chem.* **1975**, *14*, 2327.
(17) Balch, A. L.; Sohn, Y. S. *J. Am. Chem. Soc.* **1971**, *93*, 1290.
(18) Ghedini, M.; Dolcetti, G.; Giovannitti, B.; Denti, G. *Inorg. Chem.* **1977**, *16*, 1725.
(19) Balch, A. *J. Am. Chem. Soc.* **1973**, *95*, 2723.
(20) Razunaev, G. A.; Abakumov, G. A.; Teplova, I. A.; Shalnova, K. G.; Chekasov, V. K. *Inorg. Chim. Acta* **1981**, *53*, L267.
(21) Fox, G. A.; Pierpont, C. G. *Inorg.Chem.* **1992**, *31*, 3718.
(22) Kamath, S. S.; Uma, V.; Srivastava, T. S. *Inorg. Chim. Acta* **1989**, *166*, 91.
(23) Kumar, L.; Puthraya, K. H.; Srivastava, T. S. *Inorg. Chim. Acta* **1984**, *86*, 173.
(24) Barbaro, P.; Claudio, B.; Linn, K.; Mealli, C.; Meli, A.; Vizza, F.; Laschi, F.; Zanello, P. *Inorg. Chim. Acta* **1992**, *198−200*, 31.
(25) Barbaro, P.; Bianchini, C.; Mealli, C.; Meli, A. *J. Am. Chem. Soc.* **1991**, *113*, 3181.
(26) Bencini, A.; Bill, E.; Mariotti, F.; Totti, F.; Scozzafava, A.; Vargas, A. *Inorg. Chem.* **2000**, *39*, 1418.
(27) Lange, C. W.; Pierpont, C. G. *J. Am. Chem. Soc.* **1992**, *114*, 6582.
(28) Lamansky, S.; Djurovich, P.; Abdel-Razzaq, F.; Garon, S.; Murphy, D. L.; Thompson, M. E. *J. Appl. Phys.* **2002**, *92*, 1570.
(29) Chen, F. C.; Yang, Y.; Thompson, M. E.; Kido, J. *Appl. Phys. Lett.* **2002**, *80*, 2308.
(30) Markham, J. P. J.; Lo, S.-C.; Magennis, S. W.; Burn, P. L.; Samuel, I. D. W. *Appl. Phys. Lett.* **2002**, *80*, 2645.
(31) Zhu, W.; Mo, Y.; Yuan, M.; Yang, W.; Cao, Y. *Appl. Phys. Lett.* **2002**, *80*, 2045.
(32) Adachi, C.; Baldo, M.; Thompson, M. E.; Forrest, S. R. *J. Appl. Phys.* **2001**, *90*, 5048.
(33) Ikai, M.; Tokito, S.; Sakamoto, Y.; Suzuki, T.; Taga, Y. *Appl. Phys. Lett.* **2001**, *79*, 156.
(34) Adachi, C.; Lamansky, S.; Baldo, M. A.; Kwong, R. C.; Thompson, M. E.; Forrest, S. R. *Appl. Phys. Lett.* **2001**, *78*, 1622.
(35) Lamansky, S.; Djurovich, P. I.; Murphy, D.; Abdel-Razzaq, F.; Lee, H. E.; Adachi, C.; Burrows, P. E.; Forrest, S. R.; Thompson, M. E. *J. Am. Chem. Soc.* **2001**, *123*, 4304.
(36) Baldo, M. A.; Thompson, M. E.; Forrest, S. R. *Nature* **2000**, *403*, 750.
(37) Baldo, M. A.; Lamansky, S.; Burrows, P. E.; Thompson, M. E.; Forrest, S. R. *Appl. Phys. Lett.* **1999**, *75*, 4.
(38) Li., J.; Djurovich, P. I.; Alleyne, B. D.; Yousufuddin, M.; Ho, N. N.; Thomas, J. C.; Peters, J. C.; Thompson, M. E. *Inorg. Chem.* **2005**, *44*, 1713.
(39) Lu, W.; Mi, B. X.; Chan, M. C. W.; Hui, Z.; Zhu, N.; Lee, S. T.; Che, C. M. *Chem. Commun.* **2002**, 206.
(40) Adachi, C.; Baldo, M. A.; Forrest, S. R.; Lamansky, S.; Thompson, M. E.; Kwong, R. C. *Appl. Phys. Lett.* **2001**, *78*, 1622.
(41) Chan, S.-C.; Chan, M. C.; Wang, Y.; Che, C. M.; Cheung, K. K.; Zhu, N. *Chem.—Eur. J.* **2001**, *7*, 4180.
(42) Kwong, R. C.; Sibley, S.; Dubovoy, T.; Baldo, M. A.; Forrest, S. R.; Thompson, M. E. *Chem. Mater.* **1999**, *11*, 3709.
(43) O'Brien, D. R.; Baldo, M. A.; Thompson, M. E.; Forrest, S. R. *Appl. Phys. Lett.* **1999**, *74*, 442.
(44) Cleave, V.; Yahioglu, G.; Barny, P. L.; Friend, R. H.; Tessler, N. *Adv. Mater.* **1999**, *11*, 285.
(45) Baldo, M. A.; O'Brien, D. F.; You, Y.; Shoustikov, A.; Sibley, S.; Thompson, M. E.; Forrest, S. R. *Nature* **1998**, *395*, 151.
(46) Kunugi, Y.; Mann, K. R.; Miller, L. L.; Exstrom, C. L. *J. Am. Chem. Soc.* **1998**, *120*, 589.
(47) Lamansky, S.; Djurovich, P.; Murphy, D.; Abdel-Razzaq, F.; Kwong, R.; Tsyba, I.; Bortz, M.; Mui, B.; Bau, R.; Thompson, M. E. *Inorg. Chem.* **2001**, *40*, 1704.
(48) Brooks, J.; Babayan, Y.; Lamansky, S.; Djurovich, P. I.; Tsyba, I.; Bau, R.; Thompson, M. E. *Inorg. Chem.* **2002**, *41*, 3055.

Experimental Details

Materials and Synthesis. Iridium(III) chloride, $IrCl_3$, and potassium tetrachloroplatinate(II), K_2PtCl_4, were used as purchased from Next Chimica. 3,5-Di-*tert*-butylcatechol (DTBCat), *p*-tolylpyridine (tpy), and tetramethylammonium hydroxide (25 wt % solution in methanol) were purchased from Aldrich Chemical Co. and used without further purification. 2,4-difluorophenylpyridine (dfppy) was synthesized by a Suzuki coupling reaction of commercially available di-fluoroboronic acid with bromopyridine. The reference dyes, IR-27 and IR-140, for near-infrared emission studies were also purchased from Aldrich Chemical Co.

(Ir-sq). The iridium(III) μ-dichloro-bridged dimer, $[Ir(C\hat{}N)_2(\mu\text{-}Cl)]_2$, was made by thermal coupling of Ir(III) chloride ($IrCl_3 \cdot nH_2O$) salt with a slight excess of 2 equiv of *p*-tolyl pyridine (tpy) in a 3:1 mixture of ethoxyethanol and water at 80 °C. The mixture was refluxed overnight, and the yellow precipitate of the product was filtered, washed, and dried.

3,5-Di-*tert*-butylcatechol (3,5-DTBCat) was coupled to the chloro-bridged iridium dimer in the presence of the base, tetramethyl ammonium hydroxide. To a solution of the dimer and a slight excess of 3,5-DTBCat in dichloroethane/ethanol (5:1), the base was added dropwise while purging with nitrogen. The color changed gradually from yellow to olive green. The mixture was stirred at room temperature and exposed to air for about 1 h. The stirring was stopped after 3 days, and the solvent was evaporated. The product was purified by silica gel column chromatography using dichloromethane as solvent.

The pure complex was isolated as an olive-green solid in about 90% yield. FAB^+-MS (*m*/*z*): 749.27. Elemental analysis: C 61.18, H 5.46, N 3.66 (found); C 60.94, H 5.38, N 3.74 (calcd). ^{1}H NMR (250 MHz, in *d*-$CHCl_3$): broad signals in aromatic and aliphatic regions. Some of it was sublimed at about 220 °C in vacuum.

(Pt-sq). Platinum(II) monochloro complex [Pt(C^N)(HC^N)(Cl)] was made as above by thermal coupling of potassium tetrachloroplatinate (K_2PtCl_4) salt with 2,4-diflorophenylpyridine (dfppy).[49] The light-yellow precipitate of the product was filtered, washed, and dried.

3,5-Di-*tert*-butylcatechol was coupled to the above complex in the presence of the base, tetramethyl ammonium hydroxide. To a solution of the monochloro complex and a slight excess of the catechol ligand in a 5:1 mixture of 1,2-dichloroethane and ethanol, the base was added dropwise while purging with nitrogen. The color changed gradually from yellow to olive green. The mixture was stirred at room temperature and exposed to air for about 1 h. The stirring was stopped after 3 days, and the solvent was evaporated. The product was purified by silica gel column chromatography using dichloromethane as solvent.

The pure complex was isolated as a green-brown solid in about 90% yield. EIMS *m*/*z:* 605. Elemental analysis: C 49.37, H 3.98, N 2.33 (found); C 49.59, H 4.33, N 2.31 (calcd). ^{1}H NMR (250 MHz, in *d*-$CHCl_3$): broad signals in aromatic and aliphatic regions.

Spectroscopic Measurements. ^{1}H NMR spectra were recorded on a Bruker AC 250 MHz instrument. The elemental analysis was done at the Microanalysis Laboratory at the University of Illinois, Urbana-Champaign. The mass spectrometry for the Ir-sq complex in the FAB ionization mode was performed at California Institute of Technology, Pasadena, on a JEOL machine using nitrooctophenyl ether as the matrix. The solid-probe mass spectrum for the Pt-sq complex was taken with a Hewlett-Packard GC/MS instrument with electron impact ionization and a model 5973 mass-selective detector.

EPR spectra were recorded using an X-band Bruker EMX spectrometer (controlled by Bruker Win EPR Software, version 3.0) equipped with a rectangular cavity working in the TE_{102} mode. Low-temperature measurements at 80 K were conducted with an Oxford continuous-flow helium cryostat (temperature range 3.6−300 K). All of the spectra were acquired in toluene solution.

The UV−visible absorption spectra were recorded at room temperature in dichloromethane solution on a Hewlett-Packard 4853 diode array spectrophotometer. The near-infrared absorption spectra were recorded at room temperature in dichloromethane solution on a Nicolet 860 Magna Series FTIR using a quartz beam splitter and a DTGS-KBr detector. Steady-state emission spectra were measured using a Photon Technology International QuantaMaster C-60 spectrofluorimeter. The room-temperature measurements in solution were recorded in dichloromethane and in 2-methyltetrahydrofuran that was freshly distilled over sodium. The low-temperature (77 K) measurements were taken only in the 2-methyltetrahydrofuran solutions. The solutions were degassed under nitrogen before measurement. Solutions of IR-27 and IR-140 in dichloromethane were used as a reference in the near-infrared region.

X-ray Diffraction Methods. Diffraction data for the iridium complex (Ir-sq) were collected on a Bruker SMART APEX CCD diffractometer with graphite-monochromated Mo Kα radiation (λ = 0.71073 Å). The cell parameters were obtained from the least-squares refinement of the spots (from 60 collected frames) using the SMART program. A hemisphere of the crystal was collected at a resolution up to 0.75 Å, and the intensity data were processed using the SAINT-Plus program. All of the calculations for structure determination were carried out using the SHELXTL package (version 5.1). Initial atomic positions were located by Patterson methods using XS, and the structures were refined by least-squares methods using SHELX 93 with 7149 independent reflections within the range of ϕ = 1.60 to 27.49 (completeness 93.7%). Empirical absorptions were applied using SADABS. Calculated hydrogen positions were input and refined in a riding manner along with the attached carbons. A summary of the refinement details and the resulting factors are given in the Supporting Information.

Diffraction data for the platinum complex (Pt-sq) were collected on a Bruker Kappa/ApexII system equipped with graphite monochromated Mo radiation. The data crystal was mounted using oil (Paratone-N, Exxon) to a 0.3 mm cryoloop (Hampton Research) with the (0, 1, −1) scattering planes roughly normal to the spindle axis. All of the crystals examined exhibited non-merohedral twinning (roughly imposing a pseudo 2-fold along the *a* axis). Two distinct cells were identified using APEX2 (Bruker, 2004) and Cell_Now (Sheldrick, 2004). Four frame series were integrated and filtered for statistical outliers using SAINT (Bruker, 2001) and then corrected for absorption by integration using SHELXTL/XPREP (Bruker, 2001) before using SAINT/TWINABS (Bruker, 2001) to sort, merge, and scale the combined data. Combined unit-cell parameters were determined from both components using SAINT (Bruker, 2001). The twin law by rows was (1, 0, 0.296), (0, −1, 0), (0, 0, −1). Non-overlapping reflections from the primary orientation were used for phasing. Combined data with complete or no overlap were used for refinement. No decay correction was applied.

The structure was phased by dual space methods (Schneider, 2002). Systematic conditions suggested an ambiguous space group. The space-group choice was confirmed by successful convergence of the full-matrix least-squares refinement on F^2^. The highest peaks in the final difference Fourier map were in the vicinity of atoms C21_1, C1_3, and C6_2; the final map had no other significant features. A final analysis of variance between observed

(49) Cho, J. Y.; Suponitsky, K. Y.; Li, J.; Tirnofeeva, T. V.; Barlow, S.; Marder, S. R. *J. Organomet. Chem.* **2005**, *690*, 4090.

and calculated structure factors showed little dependence on amplitude or resolution; however, reflections in the h1l planes were sensitive to minor changes in the proposed model. A summary of the refinement details and the resulting factors are given in the Supporting Information.

Electrochemical Methods. Cyclic voltammetry and differential-pulsed voltammetry were performed using an EG&G potentiostat/galvanostat 283. Anhydrous acetonitrile (Aldrich) was used as solvent under a nitrogen atmosphere, and 0.1 M tetra(*n*-butyl)-ammonium hexafluorophosphate (Aldrich) was used as the supporting electrolyte. A glassy carbon rod was used as the working electrode, a platinum wire was used as the counter electrode, and a silver/silver chloride microelectrode was used as the reference electrode.

Theoretical Methods. Geometry optimizations were performed using the hybrid DFT functional B3LYP as implemented by the Jaguar 6.0 program package.[50] This DFT functional utilizes the Becke three-parameter functional[51] (B3) combined with the correlation functional of Lee, Yang, and Par[52] (LYP), and is known to produce good descriptions of reaction profiles for transition-metal-containing compounds.[53,54] The metals were described by the Wadt and Hay[55−57] core-valence (relativistic) effective core potential (treating the valence electrons explicitly) using the LACVP basis set with the valence double-ζ contraction of the basis functions, LACVP**. All of the electrons were used for all of the other elements using a modified variant of Pople's[58,59] 6-31G** basis set, where the six d functions have been reduced to five. All of the DFT calculations were calculated as unrestricted doublets.

Excited states were investigated theoretically using time dependent DFT (TD-DFT) calculations with the Gaussian 03 program.[60] To investigate the low-energy excitations in the Pt and Ir complexes, TD-DFT calculations were performed using the B3LYP hybrid functional[51,52] together with the standard LanL2DZ basis set and ECP specification, which uses the D95V valence double-ζ basis set[61] for the light elements and the Los Alamos ECP plus DZ[55] on the metals.

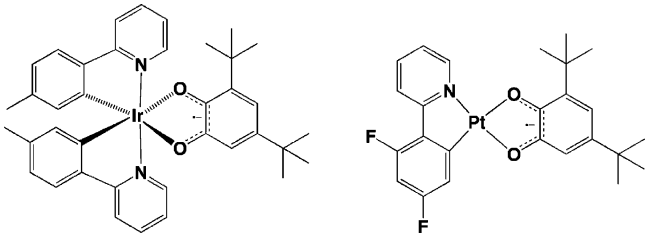

Ir-sq Pt-sq

Figure 1. Chemical structures of iridium and platinum complexes. The structural isomer of Pt-sq, where the catechol ligand is rotated 180°, is referred to as Pt-sq$_2$.

Results and Discussion

Synthesis and Characterization. The C^N chloride complexes of Ir and Pt were treated with a base and 3,5-di-*tert*-butylcatechol (3,5-dtbcat) to form the dark-colored complexes of the dioxolene ligand. The reaction was carried out under nitrogen to avoid oxidation of the deprotonated catechol species. The organic base tetramethyl ammonium hydroxide [N(Me)$_4$OH] has good solubility in methanol and is thereby miscible with the catechol in solution. This avoids the use of thallium acetate that has previously been used for the synthesis of ruthenium−dioxolene complexes.[15] The dark-green to black metal complexes of both platinum and iridium were worked up and purified in ambient conditions and are found to be stable. The iridium complex is sublimable under vacuum at about 220 °C.

The crystals for both of the compounds were grown at room temperature over a period of one week by diffusion of hexane into a dichloromethane solution. The Ir-sq crystals are olive green in color and prismatic in shape, whereas the Pt-sq crystals are green and brown and platelike in appearance.

The structures of both Ir-sq and Pt-sq were determined by X-ray crystallography. The thermal ellipsoid views of the metal complexes are shown in Figure 2. The C−O bond lengths in the semiquinone ligand of the two complexes are 1.28−1.30 Å (C1−O1 = 1.295(5) and 1.285(7) Å, C2−O2 = 1.291(5) and 1.296(7) Å for Ir-sq and Pt-sq, respectively). This bond distance is consistent with the C−O length found in the semiquinone ligand in a large number of quinone complexes.[6] The six-carbon ring (C1 through C6) has nonaromatic character with bond distances consistent with other metal complexes of the same semiquinone ligand.[21,62] The C1−C2 bond length within the chelate ring is 1.447(6) Å for Ir-sq and 1.444(7) Å for the Pt-sq complex. This bond distance corresponds to the semiquinone form of the ligand in comparison to the 1.40 Å bond length for the same two carbons in a catecholate ligand.[6]

In the Pt-sq complex, mirror symmetry was imposed on two independent molecules separated by one half of a unit-cell length along the unique *b* axis (Figure 2). The stacked dimers have an interplanar spacing of 3.4 Å, whereas the closest Pt−Pt distance is 3.47 Å. The metal−metal interac-

(50) *Jaguar 5.0*; Schrodinger, Inc.: Portland, OR, 2000.
(51) Becke, A. D. *J. Chem. Phys.* **1993**, *98*, 5648.
(52) Lee, C.; Yang, W.; Parr, R. G. *Phys. Rev. B* **1988**, *37*, 785.
(53) Baker, J.; Muir, M.; Andzelm, J.; Scheiner, A. *Chemical Applications of Density-Functional Theory*; American Chemical Society: Washington, DC, 1996.
(54) Niu, S.; Hall, B. M. *Chem. Rev.* **2000**, *100*, 353.
(55) Hay, P. J.; Wadt, W. R. *J. Chem. Phys.* **1985**, *82*, 299.
(56) Goddard, W. A., III. *Phys. Rev.* **1968**, *174*, 659.
(57) Melius, C. F.; Olafson, B. O.; Goddard, W. A., III. *Chem. Phys. Lett.* **1974**, *28*, 457.
(58) Hariharan, P. C.; Pople, J. A. *Chem. Phys. Lett.* **1972**, *16*, 217.
(59) Francl, M. M.; Pietro, W. J.; Hehre, W. J.; Binkley, J. S.; Gordon, M. S.; DeFrees, D. J.; Pople, J. A. *J. Chem. Phys.* **1982**, *77*, 3654.
(60) Frisch, M. J.; Trucks, G. W.; Schlegel, H. B.; Scuseria, G. E.; Robb, M. A.; Cheeseman, J. R.; Montgomery, J. A., Jr.; Vreven, T.; Kudin, K. N.; Burant, J. C.; Millam, J. M.; Iyengar, S. S.; Tomasi, J.; Barone, V.; Mennucci, B.; Cossi, M.; Scalmani, G.; Rega, N.; Petersson, G. A.; Nakatsuji, H.; Hada, M.; Ehara, M.; Toyota, K.; Fukuda, R.; Hasegawa, J.; Ishida, M.; Nakajima, T.; Honda, Y.; Kitao, O.; Nakai, H.; Klene, M.; Li, X.; Knox, J. E.; Hratchian, H. P.; Cross, J. B.; Bakken, V.; Adamo, C.; Jaramillo, J.; Gomperts, R.; Stratmann, R. E.; Yazyev, O.; Austin, A. J.; Cammi, R.; Pomelli, C.; Ochterski, J. W.; Ayala, P. Y.; Morokuma, K.; Voth, G. A.; Salvador, P.; Dannenberg, J. J.; Zakrzewski, V. G.; Dapprich, S.; Daniels, A. D.; Strain, M. C.; Farkas, O.; Malick, D. K.; Rabuck, A. D.; Raghavachari, K.; Foresman, J. B.; Ortiz, J. V.; Cui, Q.; Baboul, A. G.; Clifford, S.; Cioslowski, J.; Stefanov, B. B.; Liu, G.; Liashenko, A.; Piskorz, P.; Komaromi, I.; Martin, R. L.; Fox, D. J.; Keith, T.; Al-Laham, M. A.; Peng, C. Y.; Nanayakkara, A.; Challacombe, M.; Gill, P. M. W.; Johnson, B.; Chen, W.; Wong, M. W.; Gonzalez, C.; Pople, J. A. *Gaussian 03*, revision C.02; Gaussian, Inc.: Wallingford, CT, 2004.
(61) Dunning, T. H., Jr.; Hay, P. J. *Modern Theoretical Chemistry*; Plenum: New York, 1976; Vol. 3, pp 1−28.
(62) Bone, S. R.; Pierpont, C. G. *Inorg. Chem.* **1987**, *26*, 1769.

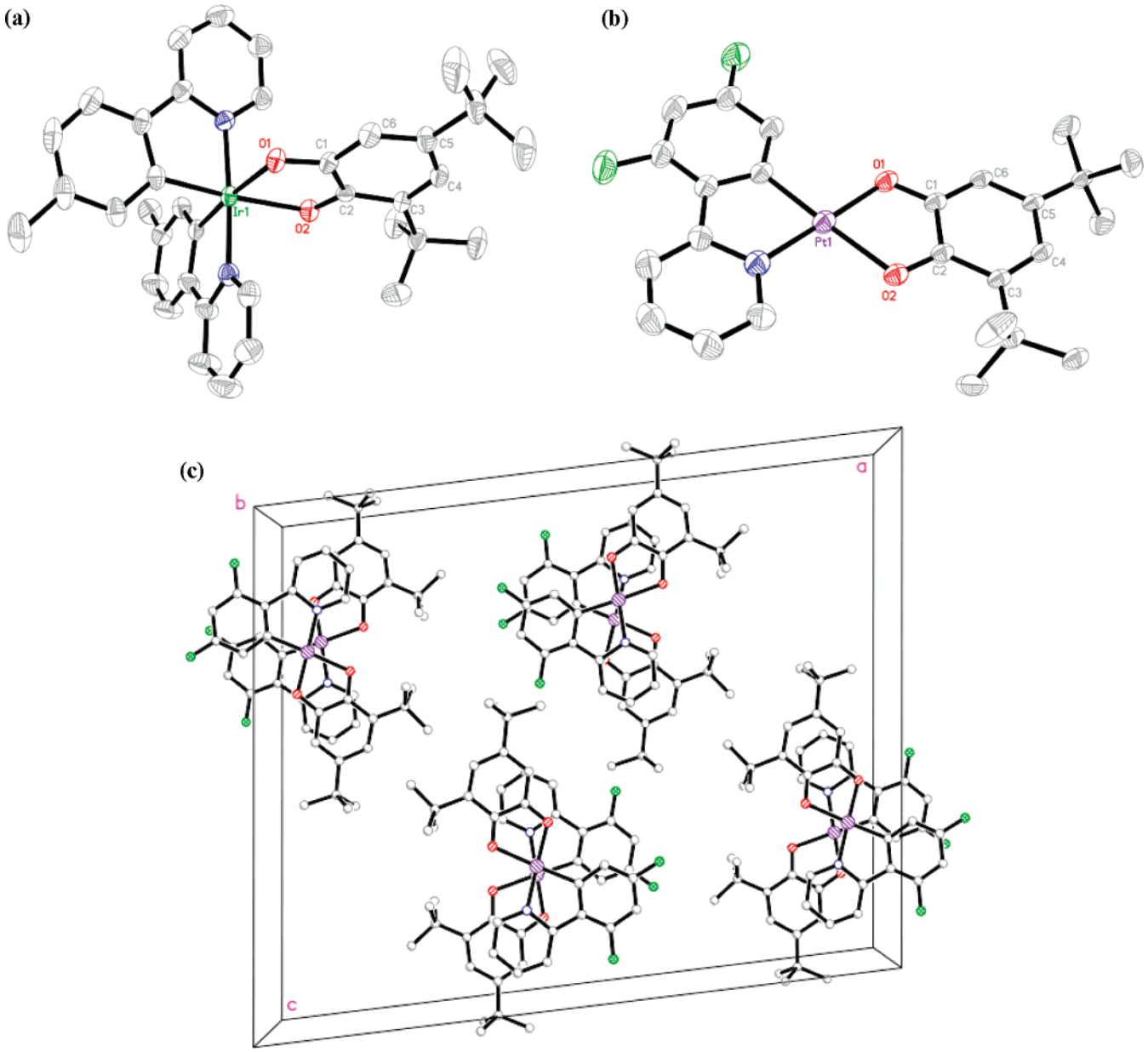

Figure 2. Thermal ellipsiodal views of (a) the Ir-sq complex and (b) the Pt-sq complex. Also shown is the packing diagram (c) of Pt-sq in a unit cell.

tion in the crystal is very weak; however, similar structures in related Pt(II) complexes lead to dimer or excimer structures in their excited state.[63−71]

(63) Ma, B.; Li, J.; Djurovich, P.; Yousufuddin, M.; Bau, R.; Thompson, M. E. *J. Am. Chem. Soc.* **2005**, *127*, 28−29.
(64) Yam, V. W.-W.; Wong, K. M.-C.; Zhu, N. *J. Am. Chem. Soc.* **2002**, *124*, 6506−6507.
(65) Lai, S.-W.; Lam, H.-W.; Lu, W.; Cheung, K.-K.; Che, C.-M. *Organometallics* **2002**, *21*, 226−234.
(66) Yersin, H.; Dinges, D.; Humbs, W.; Strasser, J.; Sitters, R.; Glasbeek, M. *Inorg. Chem.* **2002**, *41*, 4915.
(67) Miskowski, V. M.; Houlding, V. H. *Inorg. Chem.* **1989**, *28*, 1529−1533.
(68) Connick, W. B.; Marsh, R. E.; Schaefer, W. P.; Gray, H. B. *Inorg. Chem.* **1997**, *36*, 913−922.
(69) Bailey, J. A.; Hill, M. G.; Marsh, R. E.; Miskowski, V. M.; Schaefer, W. P.; Gray, H. B. *Inorg. Chem.* **1995**, *34*, 4591−4599.
(70) Buchner, R.; Cunningham, C. T.; Field, J. S.; Haines, R. J.; McMillin, D. R.; Summerton, G. C. *J. Chem. Soc., Dalton Trans.* **1999**, 711−717.
(71) Lai, S.-W.; Chan, M. C.-W.; Cheung, T.-C.; Peng, S.-M.; Che, C.-M. *Inorg. Chem.* **1999**, *38*, 4046.

EPR Spectra. Previous reports of metal complexes of platinum and iridium with the dioxolene ligand show that they are EPR active, with g values close to that of a free electron.[22−25] Both of the compounds, Ir-sq and Pt-sq, as isolated in ambient conditions, appear as a sharp radical signal centered at $g = 1.987$ and 2.003, respectively, in the room-temperature EPR spectra in toluene. This leads us to conclude that the compounds are paramagnetic in nature and that the catechol ligand is in the semiquinone form as a radical anion. The g values are comparable to those observed for other platinum- and iridium-dioxolene complexes.

The heavy-metal complexes of platinum, iridium, ruthenium, and osmium exhibit anisotropy that is observed at low temperatures. The reported line width from peak to peak is less than 10 G.[19] Most of them do not show any coupling features expected from hyperfine splitting caused by the interaction of the unpaired electron with the metal nucleus.

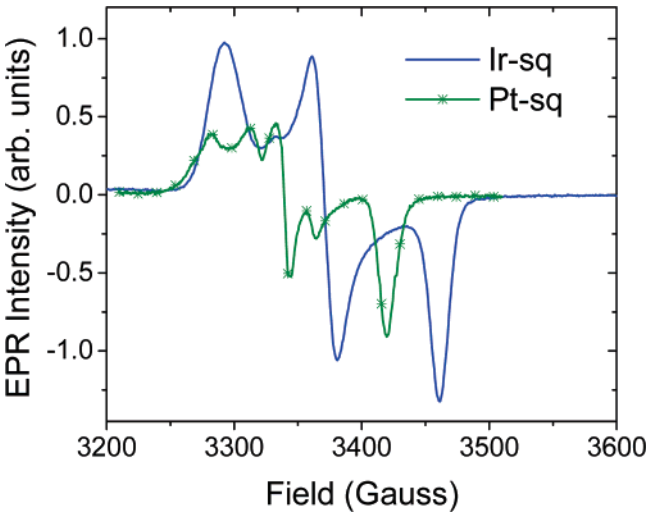

Figure 3. Low-temperature EPR spectra of the iridium and platinum complexes measured at 80 K in glassy toluene.

Table 1. Electronic Spectra and Electrochemical Data of Ir-sq and Pt-sq

sample	electronic spectra[a]	electrochemical potentials
	λ_{max}/nm (ϵ/10^{-3} $M^{-1}cm^{-1}$)	(V vs Fc^+/Fc)[b]
Ir-sq	267 (36.7), 313 (21.2), 408 (4.27), 594 (3.07)	−2.68, −0.88, +0.08[qr], +0.90[c, ir]
Pt-sq	248 (30.2), 281 (15.2), 442 (6.00), 522 (3.05), 648 (3.08)	−2.34, −0.46, +0.34[qr]

[a] Dichloromethane solution, the molar absorption coefficients (ϵ) are given in parentheses, and the measurements were made at room temperature. [b] The potential reported here is the average of anodic and cathodic peak potentials for a reversible process or the peak potential for an irreversible process. Unless otherwise noted, the redox process is reversible. qr: quasi-reversible; ir: irreversible. [c] Oxidation potential for the disolvento complex of iridium.

There is no detectable coupling even to phosphorus atoms in compounds of platinum and iridium with triphenylphosphines and 1,2-dioxolene type ligands,[16,24] consistent with preferential localization of the unpaired electron on the semiquinone ligand. The ruthenium complex[14] $(bpy)_2$Ru(dtbsq) shows axially symmetric EPR at 77 K that lead the authors to conclude that the molecular orbital containing the unpaired electron is partially localized on the metal. In the related osmium complex[13] $(bpy)_2$Os(dtbsq), rhombic structure associated with low-spin d^5 Os(III) in an octahedral environment is reported from the EPR spectrum at 77 K. Two components at $g_1 = 2.448$ and $g_2 = 1.71$ are seen, but g_3, the third component at high field, is reported unobserved. Hyperfine coupling is not observed for these ruthenium or osmium complexes.

At 80 K, in glassy toluene, a rhombic spectrum (Figure 3) is obtained for Ir-sq with $g_1 = 2.035$, $g_2 = 1.987$, and $g_3 = 1.935$ with peak-to-peak separation of about 10 G. The parameters for Pt-sq (Figure 3) are $g_1 = 2.042$, $g_2 = 2.006$, and $g_3 = 1.958$. The anisotropy reflects lower symmetry of the electronic environment around the metal centers. The g value and the small g spread indicate that the p orbital contribution from the ligand is greater than that of the d orbital from the metal, and thus, the unpaired electron is localized mainly on the ligand. Low-spin d^5 metal complexes exhibit larger anisotropy, with a large g spread, than the

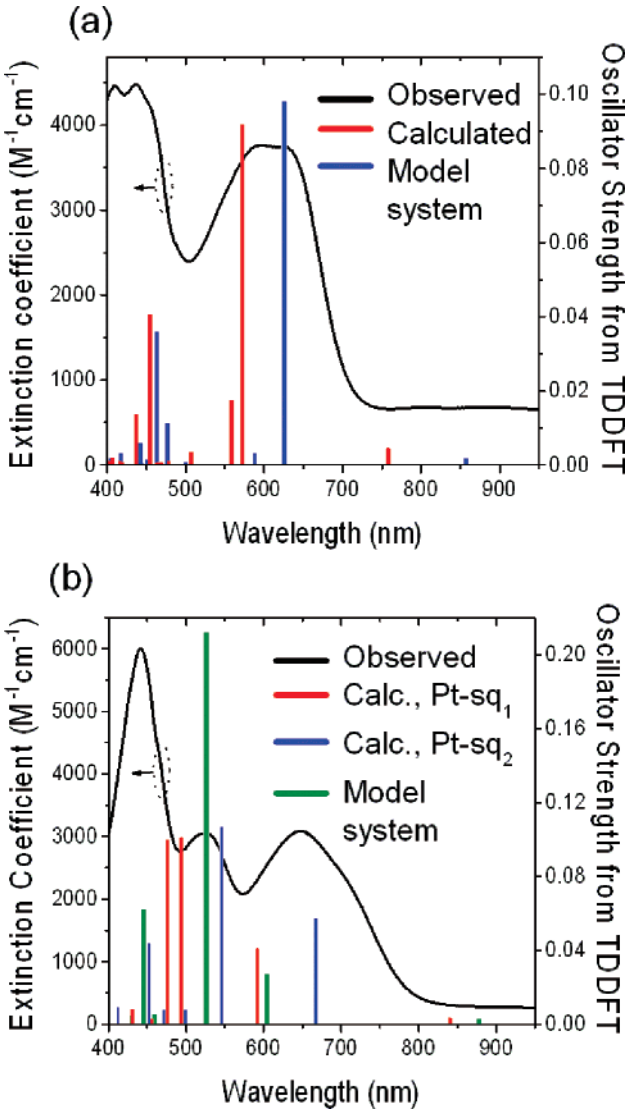

Figure 4. Electronic spectra of (a) Ir-sq and (b) Pt-sq complexes measured in dichloromethane at room temperature. The molar absorbance is in units of $M^{-1}cm^{-1}$. The calculated transition energies (from TD-DFT) are shown as bars.

values observed here.[72] The line width corresponds to that observed for other iridium(III) and platinum(II) complexes[19] of dioxolene-type ligands.

No resolvable hyperfine features are observed. The hyperfine splitting is not seen, neither from the proton at C-4 of the *o*-semiquinone ligand nor from the metal nuclei (^{191}Ir or ^{193}Ir, $I = {}^3/_2$; ^{195}Pt, $I = {}^1/_2$). This agrees with the previously reported absence of coupling features in similar metal complexes.

The symmetry observations from EPR spectra suggest that the ground-state electronic structures of both Ru and Os complexes have a contribution from the metal orbitals, but it is greater in the Os complex than in the Ru complex. Similarly, we can say that mixing metal and ligand orbitals in both the iridium and the platinum complexes results in delocalization of the unpaired electron that gives them a mixed ground-state electronic structure but with the unpaired electron being localized mainly on the ligand.

(72) Hudson, A.; Kennedy, M. J. *J. Chem. Soc. A* **1969**, 1116.

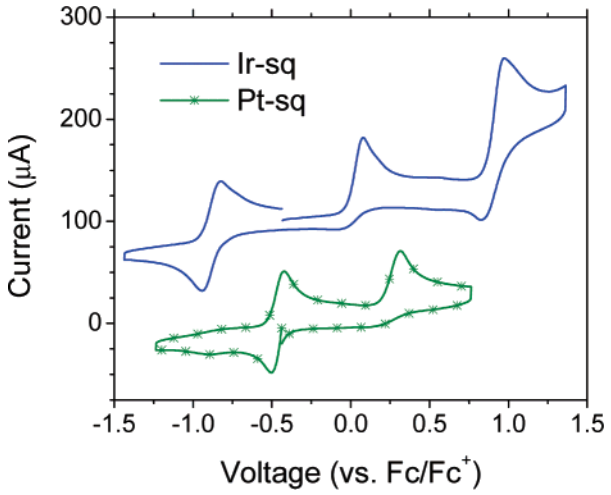

Figure 5. Cyclic voltammograms of Ir-sq and Pt-sq complexes measured in acetonitrile at room temperature. The potentials are shown relative to the internal reference couple Fc^+/Fc. TBAP (0.1 M) was used as the supporting electrolyte.

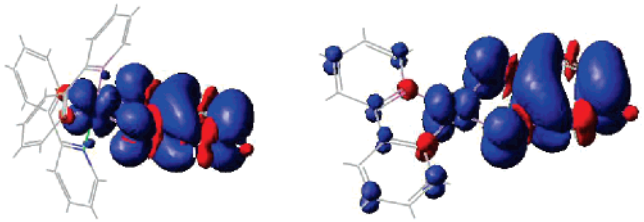

Figure 6. Spin densities calculated from the density functional theory method for the Ir-sq (left) and Pt-sq (right) complexes. The substituents are not shown, for easier visualization. About 5% of the spin density resides on the metal center with the rest almost exclusively on the semiquinone ligand. Full spin density distributions can be found in the Supporting Information.

Electronic Spectra. The absorption spectra of both the iridium and the platinum complexes show intense bands in the ultraviolet region between 250 and 350 nm. These high-energy bands can be assigned primarily to the allowed $^1(\pi-\pi^*)$ transitions of the C^N cyclometalating ligand.[47] The molar absorptivity (Table 1) is higher for the iridium complex than for the platinum complex because of the presence of twice the number of C^N ligands in the iridium complex. The lower-energy transitions in the visible to near-infrared region of the spectra are about an order of magnitude less intense than the higher-energy ones, $\sim 10^3$ M^{-1} cm^{-1}. The visible to near-infrared region can be assigned as consisting of the MLCT (metal-to-ligand charge transfer) transition bands. The low-energy transition peaked between 600 and 650 nm is intense and broad. A weak, broad band also extends to 1200 nm in the near-infrared region. The semiquinone ligand (3,5-dtbsq) itself gives a similar spectrum. A broad low-energy transition centered at 650 nm (ϵ_{max} of about 500 M^{-1} cm^{-1}) is observed in the spectrum of 3,5-di-*tert*-butyl-*o*-benzosemiquinone in a basic DMF solution.[73] The coupling of the ligand to the metal complex increases the intensity of absorption in this region because of greater charge transfer caused by the mixing of metal and ligand orbitals (molecular modeling study below).

(73) Stallings, M. D.; Morrison, M. M.; Sawyer, D. T. *Inorg. Chem.* **1981**, *20*, 2655.

Scheme 2

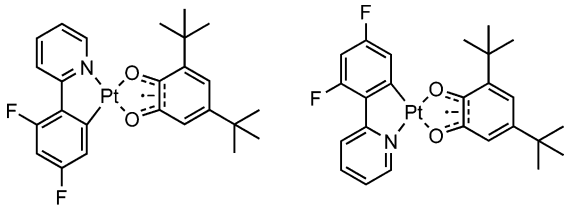

Both of the semiquinone complexes reported here were examined for photoluminescence at room temperature and at 77 K in 2-methyltetrahydrofuran. No visible emission is observed in the visible or near-infrared region at any temperature.

Electrochemistry. The electrochemical properties of the complexes were examined using cyclic voltammetry and differential-pulse voltammetry, and the data are summarized in Table 1. The potentials that are reported here were measured relative to a standard Ag/AgCl reference electrode and are adjusted to internal ferrocene reference (Fc^+/Fc measured 0.436 V versus Ag/AgCl) for reporting in literature.

The Ir-sq complex shows four redox couples in the range of −2.5 to +1.5 V (versus the Fc^+/Fc couple). Part of the cyclic voltammogram is shown in Figure 5. The dioxolene ligand is in the semiquinone oxidation state at the beginning of the experiment. The most-negative couple at −2.68 V (not shown in Figure 5) has been observed from our studies of related complexes with the same C^N ligands[28,47] and has been assigned as the reduction potential for the metal bound tpy ligand. The other negative redox peak at −0.88 V is a fully reversible one-electron process. It is attributed to the catechol/semiquinone couple. The analogous ruthenium complex $Ru(bpy)_2$(dtbcat) shows this couple at −0.91 V versus Fc^+/Fc in dichloroethane.[14] The semiquinone/catechol couple for the ligand, 3,5-di-*tert*-butylcatechol in the same solvent, acetonitrile is observed at −1.75 V (vs Fc^+/Fc).[73]

The positive potential process at +0.08 V for Ir-sq is quasi-reversible. This implies that the oxidation of the semiquinone form of the ligand to the quinone form leaves it unstable in the medium and leads to the formation of some other species. This new species grows in on repeated cycling. The ligand-based redox couples are observed even on multiple cycles. This kind of slow decomposition pathway has been observed at room temperature in metal−catecholate complexes.[24−26] The unstable quinone form results in the formation of a disolvento complex of acetonitrile and a free quinone (Q). The chemical process responsible for this decomposition in $[(triphos)M^{III}(DTBCat)]^{3+}$, where M = Ir, Rh, Co, accelerated with an increase in temperature and was not observed at low temperatures.

$$[(typ)_2Ir^{III}(dtbq)] \xrightarrow{MeCN} [(tpy)_2Ir^{III}(NCMe)_2]^+ + Q$$

The most-positive couple observed at a potential of +0.90 V is reversible in Ir-sq. It relates to the oxidation of the bis-acetonitrile−iridium moiety in the solvent-coordinated cationic species. It could correspond to the Ir(III)/Ir(IV) couple.

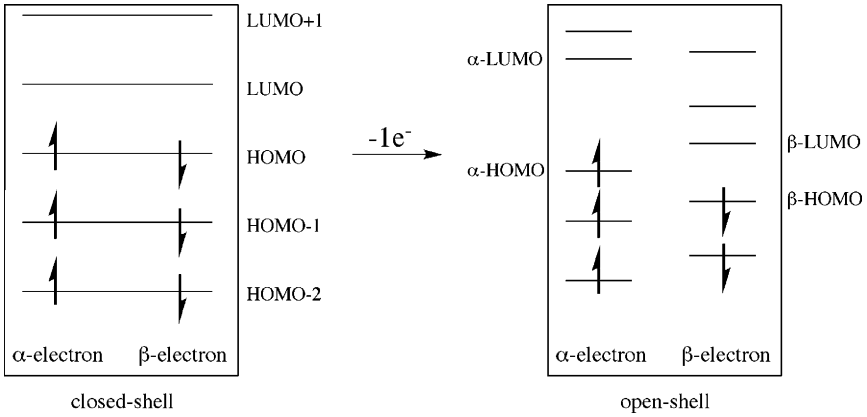

Figure 7. Naming scheme used in this work for open-shell molecules.

Similar data is observed for cyclic voltammetry on the Pt-sq complex. The separation in the two ligand-based couples is about 0.8 V for the Pt complex versus 0.96 V for the Ir complex. This separation is about 0.8 V in the electrochemical process of the ligand 3,5-di-*tert*-butylcatechol (3,5-DTBCat).[73] Because the oxidation of complexes is irreversible, this difference is not a clear measure of the HOMO−LUMO energy gap. In contrast to the Ir complex, Pt-sq does not appear to form a new species on oxidation, or one that does not have observable electrochemistry. The square-planar Pt(III) metal center is highly susceptible to nucleophilic attack by solvent, making the Pt(II/III) couple irreversible. Both the Pt(II/III) and the sq/q oxidations could be occurring under our conditions, both of which are expected to lead to rapid ligand substitution and complex degradation. The most-negative reduction potential (−2.34 V) involves reduction of the cyclometalating ligand and falls at a less-negative potential than the same reduction for Ir-sq. This is due to the presence of two electron-withdrawing fluorine atoms on the C^N ligand of Pt-sq, facilitating its reduction.

The addition of ferrocene (as an internal reference) to the solution for electrochemistry of Ir-sq results in a visible change in color, suggesting the formation of a charge-transfer complex. Cyclic voltammetry on this solution results in gradual disappearance of the previously observed redox peaks. Similar behavior is observed for Pt-sq.

DFT Calculations. Calculations were carried out on Ir-sq and on both isomers of Pt-sq (referred to as Pt-sq$_1$ and Pt-sq$_2$, Scheme 2). The results of the Pt-sq calculations showed very little difference between the two isomers, with an energy difference of only 0.1 kcal/mol. Thus, they should be considered isoenergetic within the margin of error of the calculations. The change in spin density was insignificant (root-mean-square of change = 0.01 electrons), whereas the change in orbital energies was about 1 kcal/mol on average.

Calculations were also done on the model compounds of the two complexes that use simplified (less-substituted) analogs of the metal complexes for the calculations, where the methyl or fluoro groups on the phenylpyridine moieties and the *tert*-butyl groups on the semiquinone moieties are replaced with hydrogens. This significantly reduces the size and, consequently, the computational cost of the systems. There is no significant difference in the spin density in the model systems.

The spin densities in the calculated complexes are shown in Figure 6. For both metal complexes, the spin density is centered mainly on the semiquinone ligand, only a small metal contribution. The calculated mulliken spin populations show the presence of 0.95 electrons on the semiquinone in the Ir complex and 0.94 electrons in the Pt complex. In both cases, ∼0.04 electrons reside on the metal, with the rest on the other ligands. This indicates that the metals should be considered Pt^{II} and Ir^{III} complexes with an open-shell semiquinone ligand, which supports our observations from the EPR spectra. Furthermore, the spin density is in agreement with the spin density calculated for the isolated ligand 3,5-dtbsq, located mostly on the oxygen atoms of the ligand.[74]

Molecular orbital pictures, for the Ir-sq (Figure 8) and Pt-sq (Figure 9) complexes, of the different energy levels mainly involved in the redox and excitation processes obtained by the calculations, are shown for the β electron. The difference in energy levels for the α and β electrons[75] (Figure 7) are listed in Table 2. It should be noted that the HOMO (highest occupied molecular orbital) of the α electron (the α HOMO) does not necessarily have the same symmetry as the LUMO of the β electron (the β LUMO) because of orbital reordering. Though the symmetry of the α HOMO matches that of the β LUMO in the platinum complex, this is not true in the iridium complex. In the iridium complex, the two highest-occupied α molecular orbitals (α HOMO and α HOMO-1) are nearly degenerate (the energy difference is less than 2 kcal/mol). The α HOMO corresponds in symmetry to the β HOMO, whereas the α HOMO-1 corresponds to the β LUMO.

TD-DFT Calculations. We also performed time-dependent density functional (TD-DFT) calculations on the Ir-sq and Pt-sq complexes to explain the experimentally observed electronic behavior of the two metal complexes. The transi-

(74) Wheeler, D. E.; Rodriguez, J. H.; McCusker, J. K. *J. Phys. Chem. A* **1999**, *103*, 4101.

(75) By convention, the n spin-up electrons are referred to as the α electrons, whereas the $(n - 1)$ spin-down electrons are referred to as the β electrons.

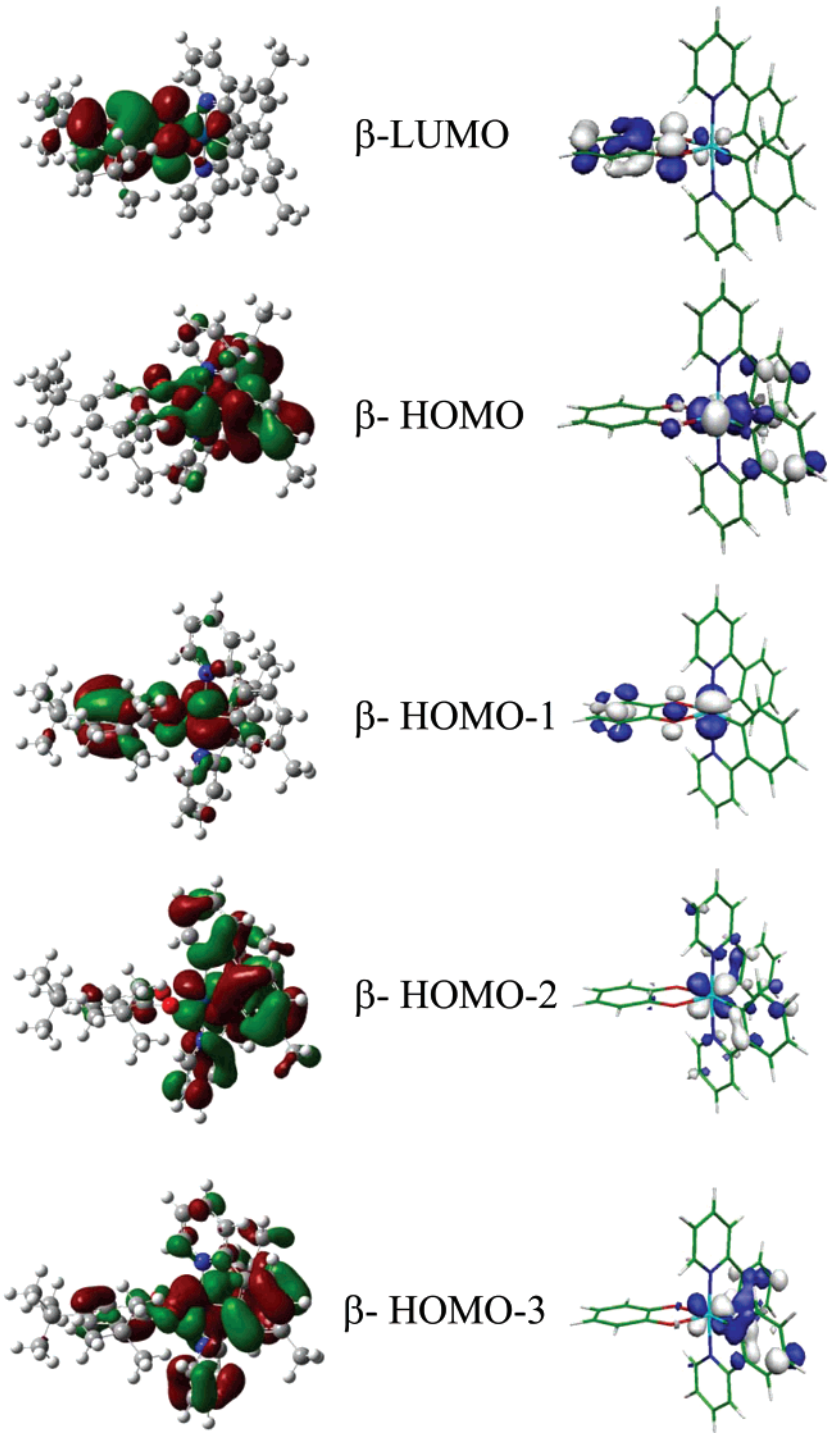

Figure 8. β molecular orbitals of Ir-sq complex obtained from TD-DFT calculations. The model (simplified) system is shown on the right.

tion energies obtained from calculations on both open-shell complexes are shown in Figure 4. The calculated absorption-peak positions are in good agreement with those in the measured spectrum for each complex. The difference in the two systems is discussed later in the section.

The calculations provide a list of the electronic transitions that contribute to each of the excited states, the oscillator strength of the transition to an excited state, and the expansion coefficient that relates to the percent contribution of the different excitations to the particular excited state (Table 3). The results show that the lowest-energy excitations come from the β molecular orbitals, in accordance with the orbital energy differences discussed above.

In the iridium complex in dichloromethane solvent, the transition at a wavelength of 571 nm is the most favorable low-energy transition with oscillator strength of about 0.09. This corresponds to the measured molar absorption maximum at 594 nm for the analogous experimental complex. The calculations show that this transition comes mainly from the β-HOMO-2 to the β-LUMO excitation. The orbital pictures

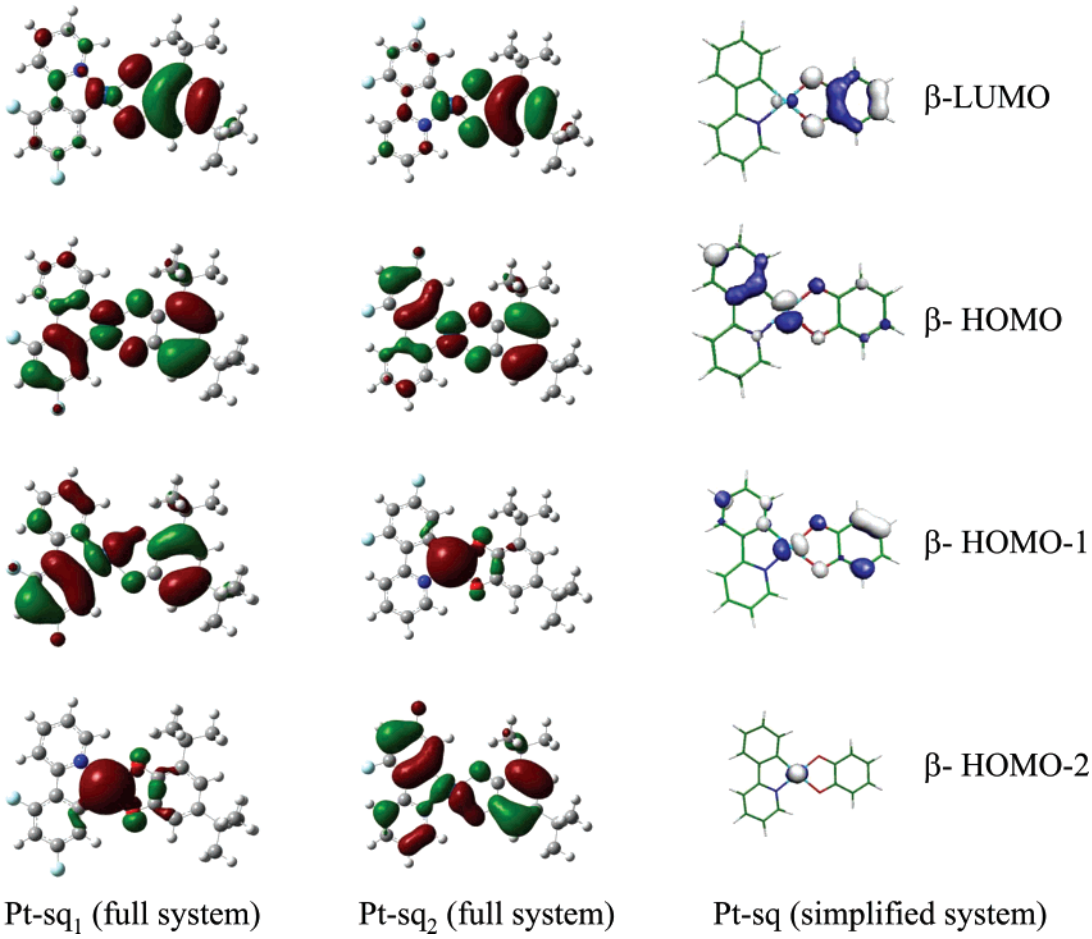

Figure 9. β molecular orbitals of Pt-sq complex obtained from TD-DFT calculations.

Table 2. Molecular Orbital Energy Differences (in kcal/mol) in the Ground State of the Ir-sq and Pt-sq$_1$ Complexes[a]

molecular orbitals of Ir-sq	ΔE for the α electron (kcal/mol)	ΔE for the β electron (kcal/mol)
E(HOMO) − E(LUMO)	77.50	48.28
E(HOMO-1) − E(HOMO)	3.81	15.17
E(HOMO-2) − E(HOMO-1)	18.88	4.13
molecular orbitals of Pt-sq	**ΔE for the α electron (kcal/mol)**	**ΔE for the β electron (kcal/mol)**
E(HOMO) − E(LUMO)	75.56	58.52
E(HOMO-1) − E(HOMO)	18.11	8.35
E(HOMO-2) − E(HOMO-1)	9.89	4.28
E(HOMO-3) − E(HOMO-2)	0.32	1.28

[a] The molecular orbitals that are involved in low-energy charge-transfer transitions (TD-DFT) are listed.

(Figure 8) show a good degree of overlap in the iridium metal d orbitals of the two molecular orbitals. Both the β HOMO and the β HOMO-1 have very poor orbital overlap with the β LUMO, and thus the excited state has almost no contribution from these excitations. This leads us to conclude that the electronic transition in the red to near-infrared region is primarily a HOMO-2 → LUMO excitation of the β electron of the iridium complex.

Theoretical calculations were done on the two structural isomers of the platinum complex in dichloromethane solvent, that is, Pt-sq$_1$ and Pt-sq$_2$. In the platinum complex, the electronic transition from the β-HOMO-1 molecular orbital to the β-LUMO molecular orbital contributes most significantly to the absorption at a wavelength of 592 nm for Pt-sq$_1$ and the β-HOMO-2 molecular orbital to the β-LUMO molecular orbital at 604 nm for Pt-sq$_2$. The β-HOMO-1 molecular orbital of Pt-sq$_1$ identifies with the β-HOMO-2 molecular orbital of Pt-sq$_2$. This excitation results from a good orbital overlap (Figure 9). Most of the electron density is centered on the semiquinone ligand, and some is centered on the metal center. For both isomers, the β HOMO has poorer orbital overlap with the β LUMO, which results in a very small percent contribution to the excited states (less than 10%). Similarly, the β HOMO-2 has almost no overlap with the β LUMO because the metal d orbitals are orthogonal to each other in the two orbitals of Pt-sq. The molecular orbital pictures that correspond to the excitation energy of transitions clearly indicate that the lowest-energy transition is a β-HOMO-1 → β-LUMO excitation or a β-HOMO-2 → β-LUMO excitation and not a HOMO → LUMO excitation (of either spin).

Another excited-state transition of significant oscillator strength was calculated at wavelengths of 494 nm ($f = 0.10$) in Pt-sq$_1$ and 526 nm ($f = 0.21$) in Pt-sq$_2$. The major contribution to this state comes from the β-HOMO-3 → β-LUMO excitation. Yet another excited-state transition (at 476 nm in Pt-sq$_1$ and at 445 nm in Pt-sq$_2$) that is of significant

Table 3. Excitations in the Ir-sq and Pt-sq Complexes that Contribute to the Charge-Transfer Transition in the Red to Near-Infrared Region along with Their Relative Contributions Given by the Expansion Coefficients[a]

	excitation wavelength (nm)	excitation energy (eV)	oscillator strength, *f*	excited state (major contribution)	expansion coefficient
Ir-sq	571.54	2.1693	0.0918	HOMO-2 → LUMO,	0.76590
				HOMO-3 → LUMO	0.51939
Ir-sq, model system	625.61	1.9818	0.0980	HOMO-2 → LUMO,	0.86547
				HOMO-3 → LUMO	0.39865
Pt-sq_1	591.77	2.0951	0.0409	HOMO-1 → LUMO	0.92845
Pt-sq_2	604.31	2.0517	0.0272	HOMO-2 → LUMO	0.90972
Pt-sq, model system	667.46	1.8576	0.0578	HOMO-1 → LUMO	0.89196

[a] The oscillator strength indicates the strqength of absorption at that wavelength.

strength (0.1 and 0.06) results mainly from an α-HOMO to α-LUMO excitation. The calculations show a weak low-energy transition in the near-infrared region for both Ir-sq (758 nm, 0.0045 oscillator strength) and Pt-sq (840 and 877 nm, 0.003 oscillator strength) complexes (Figure 4). This transition involves the β HOMO-1 and β LUMO of Ir-sq and primarily the β HOMO and β LUMO of Pt-sq. The poor orbital overlap explains the lower oscillator strength. The calculated low-energy transition corresponds to the tail of the absorption band observed in the electronic spectra of the two complexes.

It should be noted that despite minor discrepancies the calculations suggest that two isomers in the Pt-sq complex are not significantly different in their low-energy electronic excitations. Also, the model system works to a certain extent in our theoretical understanding of the electronic structure of compounds. A comparative analysis of the simplified model system with the full system suggests that the molecular orbitals that contribute significantly to the excited states are of the same density for both systems. There is a clear difference in the two systems in their calculated excitation energies in the low-energy region of the spectra. In our results on both complexes, the model system is lower in absolute energy than the full system. Nevertheless, the interpretation of the electronic structure of the complexes is the same for either system.

Thus, the theoretical calculations show that the low-energy electronic transitions observed in the open-shell iridium and platinum complexes are a result of excitations of β electrons from a HOMO-n (n is an integer, $n \geq 1$) to the LUMO. This suggests that the relaxation of the excited β electron from the LUMO into the filled molecular orbitals could occur through a series of rapid internal conversion processes, leading to no observable emission in the red to near-infrared region of the electromagnetic spectrum. Transient absorption spectroscopy of the complexes in the picosecond to femtosecond range could support the above argument.

Conclusions

A combination of experimental and theoretical approaches is used to investigate the electronic properties of iridium and platinum dioxolene complexes. The synthesis of Ir-sq and Pt-sq neutral complexes was achieved by coupling the catechol ligand to the cyclometalated complex in the presence of a base under ambient conditions. The two third-row transition-metal complexes are characterized by crystallography. The bond lengths of the catechol ligand indicate that it is in the semiquinone form in the two complexes. This observation is also supported by the electronic configuration as determined by density functional theory calculations. The low-energy transitions and the rhombic EPR spectra suggest that the unpaired electron resides mainly on the semiquinone ligand with Ir(III) and Pt(II) as the metal oxidation states. The reversible redox couple of semiquinone and catechol and the density functional theory calculations support the localization of charge on the ligand. The electrochemical oxidation results in solvent-coordinated complexes, implying the poor stability of the quinone complexes. The low-energy metal-to-ligand charge-transfer transitions calculated from time-dependent density functional theory calculations overlap fairly well with the observed absorptions of the two open-shell molecules. The calculations provide a good picture of the molecular orbitals and of the difference in orbital energies showing that the β-electron excitation is favored over the unpaired α electron in both of the complexes. This vertical excitation and a possible internal relaxation help us understand the lack of luminescence in the visible to near-infrared region of the spectrum. The rapid internal conversion observed for these complexes suggests that they will not be useful as light absorbing or sensitizing materials in solar cells because internal conversion will likely deactivate the excited state faster than charge separation.

Acknowledgment. We thank Dr. Angelo J. Di Bilio at Caltech for his help and discussion on the EPR experiments. We also thank Professor George Rossman at Caltech for measurement of the near-infrared absorption of the complexes. This research was supported by a grant from the Global Energy Photonic Corporation (GPEC).

Supporting Information Available: Crystallographic data of Ir-sq and Pt-sq complexes and tables and figures of atomic coordinates, TD-DFT calculated energies and molecular orbital compositions. This material is available free of charge via the Internet at http://pubs.acs.org.

IC061556B